


Indirect field-oriented control of induction motor drive based on adaptive fuzzy logic controller

K. Zeb¹  · Z. Ali² · K. Saleem³ · W. Uddin¹ · M. A. Javed³ · N. Christofides²

Received: 5 December 2015 / Accepted: 28 September 2016 / Published online: 13 October 2016
© Springer-Verlag Berlin Heidelberg 2016

Abstract Recently, Asynchronous Motors are extensively used as workhorse in a multitude of industrial and high-performance applications. Induction Motors (IM) have wide applications in today's industry because of their robustness and low maintenance. A smart and fast speed control system, however, is in most cases a prerequisite for most applications. This work presents a smart control system for IM using an Adaptive Fuzzy Logic Controller (AFLC) based on the Levenberg–Marquardt algorithm. A synchronously rotating reference frame is used to model IM. To achieve maximum efficiency and torque of the IM, speed control was found to be one of the most challenging issues. Indirect Field-Oriented Control (IFOC) or Indirect Vector Control techniques with robust AFLC offer remarkable speed control with high dynamic response. Computer simulation results using MATLAB/Simulink[®] Toolbox are described and examined in this study for conventional PI and AFLC. AFLC presents robustness as regards overshoot, undershoot, rise time, fall time, and transient oscillation for speed variation of IFOC IM drive in comparison with classical PI. Moreover, load disturbance rejection capability for the designed control scheme is also verified with the AFL controller.

Keywords Induction Motor (IM) · Indirect Field-Oriented Control (IFOC) · Pulse Width Modulation (PWM) ·

PI control scheme · Fuzzy Logic Controller (FLC) · Levenberg–Marquardt (LM)

1 Introduction

Three-phase Induction Motors (IM) got extensive privileged since their discovery in the industrial world, because they are inexpensive, highly efficient, modest, rugged and simple in construction, have self-starting torque, and are unsusceptible to heavy overloads [1, 2]. However, IM can become incapable for flexible speed operation because of their non-linearity and complexity which is difficult to mathematically model [3]. Speed control limitations can be overcome by implementing smart and adaptable speed controllers. Control techniques for induction motor drives are well enlightened in the literature [4, 5], with the most popular being the scalar and Vector Control (VC) methods. The classical method employed in industry is scalar control also known as Volts Hertz (V/f) control which, unfortunately, performs remarkably in the steady state. The reason for this is that the instantaneous torque control is not prominent and also does not allow flux control and decoupled torque, resulting in poor dynamic response [6]. On other hand, in Field-Oriented Control (FOC) or VC, frequency, magnitude and instantaneous position of flux linkages vectors of current and voltage are controlled. Hence, it is operative for both steady state as well as transient conditions and sanctions better dynamic performances [7].

The two main classifications of FOC schemes are: the direct and indirect technique, discovered by Blaschke in 1972 and Hasse in 1968, respectively [8, 9]. The FOC direct method tries to estimate or measure the machine flux either by interleaving flux sensors in air gap or by sensing stator voltages; however, this technique is subjected to harmonics, and is not considered beneficial at low speeds [10, 11]. On the other hand, in Indirect Field-Oriented Control (IFOC), equa-

✉ K. Zeb
kami_zeb@yahoo.com

¹ Department of Electrical Engineering, University of Management and Technology, Sialkot, Pakistan

² Department of Electrical Engineering, Frederick University, Nicosia, Cyprus

³ Department of Electrical Engineering, COMSATS Institute of Information and Technology, Abbottabad, Pakistan

tions are used to approximate the rotor flux and hence provide more accuracy over a wide speed range. Therefore, the indirect scheme is preferred over the direct scheme [12–14].

It is often challenging to continuously update the control parameters of PID family. The said classical control scheme is sensitive to irregular, unpredictable load variation, system instabilities, temperature abnormality and unavoidable parameters deviation due to saturation. The aforementioned complexity of non-linear mathematical models in conventional control approaches supports a new control strategy, hence the proposed Adaptive Fuzzy Logic Controller (AFLC) based on the Levenberg–Marquardt (LM) algorithm. AFLC has proven operative for non-linear, complex and inaccurately defined processes for which conventional control techniques are impossible and impractical [15, 16]. The AFLC embodies linguistic approach and does not necessitate any mathematical model. This subsequently makes AFLC accurate and robust to parameter variations [17–19].

This paper scrutinizes the mathematical modeling of IM and design of AFLC centered on LM technique for IFOC IM drive system. The flux weakening block is also incorporated with the IM drive for variable speed operation. IFOC using AFLC based on LM technique designed for different operating condition is implemented in Matlab/Simulink along with load variation. The load disturbance rejection capability is validated for the design control scheme. Moreover, the fallouts are critically and analytically compared with conventional PI control strategy.

The paper is organized as follows: after the introductory section, IM is mathematically modeled in Sect. 2, followed by the detailed description of proposed AFLC given in Sect. 3. Then AFLC based on LM for IFOC of IM is scrutinized in Sect. 4. Section 5 presents the simulation results of the proposed controller as compared to PI controller for three different cases, followed by conclusions and a proposal future work.

2 Induction motor modeling

Symmetrical structure, three-phase balance and linearity of rotor and stator magnetic core are assumed during derivation of dynamic modeling of IM. The modeling of IM is usually derived from voltage, flux linkage and motion equations, in synchronously rotating reference frame of both stator and rotor [20–22].

2.1 DQ reference frame

Space vector model discussed above can be easily decomposed into dq model. The dq equivalent voltage, flux linkage and motion equations can be easily achieved from space vector model by decoupling the real and imaginary part of their respective equations as shown below:

2.2 Voltage equation in dq -axis

Rotor and stator dq -axis voltages in terms of corresponding flux linkages are specified as:

$$v_{ds} = R_s I_{ds} + \frac{d\psi_{ds}}{dt} - \omega \psi_{qs} \quad (1)$$

$$v_{qs} = R_s I_{qs} + \frac{d\psi_{qs}}{dt} + \omega \psi_{ds} \quad (2)$$

$$v_{dr} = R_r I_{dr} + \frac{d\psi_{dr}}{dt} - (\omega - \omega_r) \psi_{qr} \quad (3)$$

$$v_{qr} = R_r I_{qr} + \frac{d\psi_{qr}}{dt} + (\omega - \omega_r) \psi_{dr} \quad (4)$$

v_{ds}, v_{qs} represents stator dq -axis voltages, respectively. v_{dr}, v_{qr} demonstrates rotor dq -axis voltages. Rotor and stator resistances are represented by R_s and R_r , respectively. I_{ds}, I_{qs} and I_{dr}, I_{qr} define the dq -axis stator and rotor currents, respectively. ψ_{ds}, ψ_{qs} and ψ_{dr}, ψ_{qr} represents stator and rotor dq -axis flux linkages. ω is the speed of rotation of arbitrary reference frame and ω_r is electrical speed of rotation.

2.3 Flux linkage equation in dq -axis

The flux linkage equations in the respective dq -axis equivalent equations are described as:

$$\psi_{ds} = L_s i_{ds} + L_m i_{dr} \quad (5)$$

$$\psi_{qs} = L_s i_{qs} + L_m i_{qr} \quad (6)$$

$$\psi_{dr} = L_r i_{dr} + L_m i_{ds} \quad (7)$$

$$\psi_{qr} = L_r i_{qr} + L_m i_{qs} \quad (8)$$

L_s, L_r and L_{ls}, L_{lr} are self-inductance and leakage inductance of stator and rotor, respectively, while L_m represents magnetizing inductances which are measured in Henry (H). Moreover, $L_s = L_{ls} + L_m$ and $L_r = L_{lr} + L_m$.

2.4 dq -axis model of stator and rotor

Substituting values of flux linkages in terms of inductances into voltage equations of stator and rotor, we have:

$$v_{ds} = R_s I_{ds} - \omega \psi_{qs} + L_{ls} \frac{dI_{ds}}{dt} + L_m \frac{d}{dt} (I_{ds} + I_{dr}) \quad (9)$$

$$v_{qs} = R_s I_{qs} + \omega \psi_{ds} + L_{ls} \frac{dI_{qs}}{dt} + L_m \frac{d}{dt} (I_{qs} + I_{qr}) \quad (10)$$

$$v_{dr} = R_r I_{dr} - (\omega - \omega_r) \psi_{qr} + L_{lr} \frac{dI_{dr}}{dt} + L_m \frac{d}{dt} (I_{ds} + I_{dr}) \quad (11)$$

and

$$v_{qr} = R_r I_{qr} + (\omega - \omega_r) \psi_{dr} + L_{lr} \frac{dI_{qr}}{dt} + L_m \frac{d}{dt} (I_{qs} + I_{qr}) \quad (12)$$

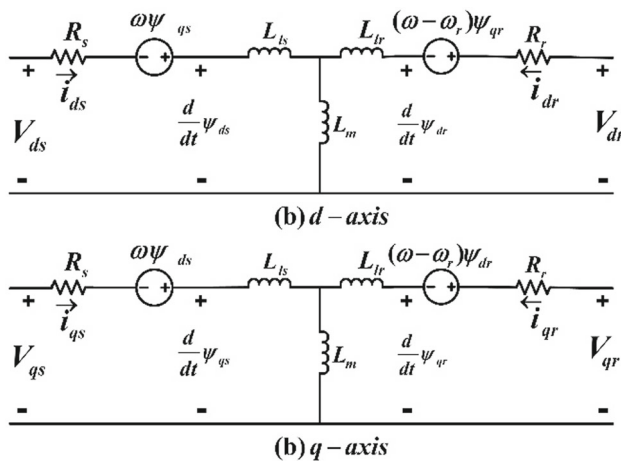


Fig. 1 dq -axis equivalent model of induction motor

2.5 Motion equation in dq -axis

Electromagnetic torque T_e can be expressed in various ways by manipulating space vector model motion equation. It can be either expressed as dq -stator and rotor current or the other way is to combine the equation of flux linkage variable of rotor and stator with dq -stator current. The frequently used equations in the literature are presented below:

$$T_e = \begin{cases} \frac{3P}{2} (i_{qs}\psi_{ds} - i_{ds}\psi_{qs}) \\ \frac{3PL_m}{2} (i_{qs}i_{dr} - i_{ds}i_{qr}) \\ \frac{3PL_m}{2L_r} (i_{qs}\psi_{dr} - i_{ds}\psi_{qr}) \end{cases} \quad (13)$$

The dq -axis equivalent model based on the above Eqs. (9)–(12) is depicted in Fig. 1.

Similarly, the final equations of electromagnetic torque and motion required for simulation are given below.

$$\begin{aligned} \frac{d\omega_r}{dx} &= \frac{P}{J} (T_e - T_m) \\ T_e &= \frac{3P}{2} (i_{qs}\psi_{ds} - i_{ds}\psi_{qs}) \end{aligned} \quad (14)$$

where J represents inertia (kgm^2) and ω_m mechanical speed (rad/s) of rotor. T_e , T_m represents electromagnetic and mechanical torque (N.m) while number of poles pair is represented by P .

3 Proposed adaptive fuzzy logic control based on LM

This section describes the detail of the proposed AFLC for the control of IM. So far, diverse controller topologies are adopted for IFOC IM drive. Every control strategy has its

own dynamics and antagonistic perspectives. None of the methodologies can coordinate the sought execution as needed by genuine plant. Fuzzy Logic Controller (FLC) is a procedure to incorporate human-like intuition into a control framework. FLC can be intended to copy human inferential considerations, that is, the methodology individuals utilizes to construct conclusions from the given stored information [23]. Experience demonstrates that utilizing FLC-based controllers has all the earmarks of being extremely valuable, specially, when the problems are too perplexing for examination by ordinary quantitative procedures or when the data are depicted subjectively, or estimated with vulnerability [24].

The performance of AFLC is highly dependent on the optimization technique used for parameter updating. Different optimization algorithms can be implemented to improve the AFLC performance. The training process of gradient descent method is particularly slow, but because of its smaller step size it always avoids saddle points, which makes it convergent [25]. If the Gauss–Newton method converges, it minimizes the residual function faster than the gradient descent method in the sense that it takes less number of iterations to reach local minimizer, but the likelihood of divergence is always there. This procedure comes up short at whatever point the Jacobian matrix's inverse does not exist [26]. LM strategy is a cross breed method which utilizes the ever convergence property of gradient descent and the quickness of Gauss–Newton method. The problem of Jacobian matrix singularity is also offset in this second-order technique [27].

In the proposed FLC, parameter updating is achieved using LM technique. The FLC versatility based on LM technique is referred to as direct adaptive control. FLC in the view of LM is best suitable technique for highly non-linear, complex system dynamics, and poorly understandable plant [28]. In an IM control framework, the purpose of FLC is to change over linguistic control rules into control methodology in view of heuristic data or master information. FLC methodology is extremely helpful for IM drives since no precise numerical model of the IM or the closed-loop framework is needed to achieve optimal system performance [23–29]. The uncertainty of non-linear model is managed by changing the center and variance of singleton membership function using knowledge-based modifier, which makes the fuzzy controller adaptive [30]. LM algorithm addresses solution to the type of problems called *Non-linear least square minimization*. The function of the form Eq. (15) is minimized by this technique [31,32].

$$f(x) = \frac{1}{2} \sum_{j=1}^m r_j^2(x) \quad (15)$$

where

$$x = [x_1 x_2 x_3 \dots x_n]^T \in R^{n \times 1} \quad (16)$$

$x \in R^{n \times 1}$ represents a vector and each r_j is the function mapping R^n to R . The r_j is the residual and it is assumed that $m \geq n$. The function r is represented as a residual vector, i.e., $r: R^n \rightarrow R^m$ defined by

$$r(x) = [r_1(x), r_2(x), \dots, r_m(x)] \quad (17)$$

The function f in Eq. (15) can be also be written as

$$f(x) = \frac{1}{2} r(x)^2 \quad (18)$$

The derivative of f can be written as the Jacobian matrix J of r with respect to x

$$J(x) = \frac{\partial r_j}{\partial x_i} \quad 1 \leq j \leq m, \quad 1 \leq i \leq n \quad (19)$$

The LM learning algorithm is given by Eq. (20).

$$\Delta w = -\lambda(J^T J + \mu I)^{-1} J e \quad (20)$$

where Δw denotes the change in update weight, J is the Jacobean matrix of r with respect to x . e denotes the error, that is, the difference between desired value and actual value. λ is used to control the step size, whereas the other parameter μ is used to make the update equation invertible and also to stabilize the algorithm [29].

The update rule for LM is given by:

$$w_{k+1} = w_k - \lambda(J_k^T J_k + \mu I)^{-1} J_k e_k \quad (21)$$

Eq. (21) is used for updating different parameters in controller design. w_{k+1} shows the updated value, w_k is the previous value, J_k is the k th Jacobean matrix, λ is combination coefficient, and I is identity matrix.

3.1 Controller design

The design of controller based on LM technique minimizes both the linear and non-linear functions and is greatly suitable for multiple input–output systems. The design comes into view from the following cost equation

$$e_m = \frac{1}{2} (f_m - y_{ref})^2 \quad (22)$$

The output equation of controller used for process of defuzzification is given by

$$f_m = \left(\sum_{i=1}^R b_i \mu_i(x_j^m, k) \right) / \left(\sum_{i=1}^R \mu_i(x_j^m, k) \right) \quad (23)$$

where

$$\mu_i(x_j^m, k) = \prod \exp\left(-\frac{1}{2} \left(\frac{x_j^m - c_j^i}{\sigma_j^i} \right)^2\right) \quad (24)$$

The input and output membership function of the fuzzy logic controller is updated using Eq. (24). σ_j^i is referred to as variance, and c_j^i is the center of the Gaussian Membership Function (GMF).

3.2 Derivation of equation for updating parameters

The error defined by Eq. (22) is used to derive the equation for updating the parameters. The derivative of Eq. (22) results in the Jacobian of each term, that is, variance, output, and center membership function.

Taking the derivative of Eq. (22) with respect to b_j

$$\frac{\partial e_m}{\partial b_j} = \frac{\partial}{\partial b_j} \left(\frac{1}{2} (f_m - y_{ref})^2 \right) \quad (25)$$

$$\frac{\partial e_m}{\partial b_j} = (f_m - y_{ref}) \frac{\partial \varepsilon}{\partial b_j} \quad (26)$$

By putting the value of f_m from Eq. (22) and $\varepsilon = (f_m - y_{ref})$ in Eq. (24), we obtain

$$\frac{\partial e_m}{\partial b_j} = \varepsilon \frac{\partial}{\partial b_j} \left[\left(\sum_{i=1}^R b_i \mu_i(x_j^m, k) \right) / \left(\sum_{i=1}^R \mu_i(x_j^m, k) \right) \right] \quad (27)$$

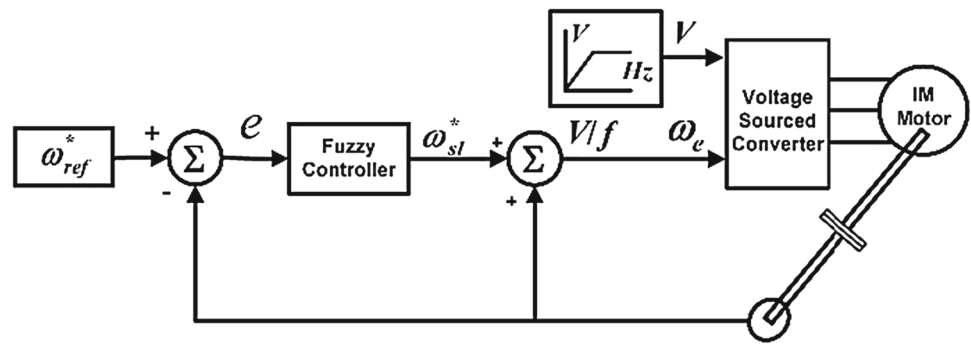
$$\frac{\partial e_m}{\partial b_j} = \varepsilon \frac{\partial}{\partial b_j} \left[\left(\sum_{i=1}^R b_i \prod \exp\left(-\frac{1}{2} \left(\frac{x_j^m - c_j^i}{\sigma_j^i} \right)^2\right) \right) / \left(\sum_{i=1}^R \prod \exp\left(-\frac{1}{2} \left(\frac{x_j^m - c_j^i}{\sigma_j^i} \right)^2\right) \right) \right] \quad (28)$$

The above Eq. (26) is the Jacobian of output membership function b_j . Likewise, taking the derivatives with respect to other variables σ_j and c_j will result in Jacobian of variance and center of membership function, respectively.

3.2.1 Update equation for output GMF

Equation (28) is used to update the output membership function, that is, output of the controller to the plant. The variable b_j denotes the center of output membership function. The center of output membership function updates in compliance with the output of the plant.

$$b_j(k+1) = b_j(k) - \lambda[A A^T + \mu I]^{-1} A \varepsilon \quad (29)$$

Fig. 2 Proposed scalar control scheme for IM

where $A = \varepsilon \left[\frac{\mu_i(x_j^m, k)}{\sum_{i=1}^R \mu_i(x_j^m, k)} \right]$

3.2.2 Update equation for variance of GMF

According to Eq. (24), the magnitude of membership function is inversely proportional to the variance. The lower value of variance results in higher membership function magnitude and vice versa. Variance characterizes the broadcast of the membership function which is updated by the following equation:

$$\sigma_j(k+1) = \sigma_j(k) - \lambda [BB^T + \mu I]^{-1} B \varepsilon \quad (30)$$

where $B = \varepsilon \left[\frac{(\sum_{i=1}^R b_i) - f_m}{\sum_{i=1}^R \mu_i(x_j^m, k)} \right] \left(\frac{(x_j^m - c_j^i)^2}{(\sigma_j^i)^3} \right) \mu_i(x_j^m, k)$

3.2.3 Update equation for center of GMF

Equation (30) updates the center of membership function. The center acquires different values in accordance with the crisp input to controller.

$$c_i(k+1) = c_i(k) - \lambda [CC^T + \mu I]^{-1} C \varepsilon \quad (31)$$

where $C = \varepsilon \left[\frac{(\sum_{i=1}^R b_i) - f_m}{\sum_{i=1}^R \mu_i(x_j^m, k)} \right] \left(\frac{(x_j^m - c_j^i)}{(\sigma_j^i)^2} \right) \mu_i(x_j^m, k)$

The design of PI controller is discussed in [20] with calculated gain values for k_p and k_i equal to 30 and 7, respectively. The initial values for parameters of AFLC based on LM are presented in Table 2. Furthermore, these parameters are randomly selected that updates itself according to Eqs. (28), (29), and (30) to minimize the error. This offers significant flexibility as the controller becomes more adaptive and robust.

4 Control schemes for IM drives

Various scalar and vector control schemes are designed for close loop IM to achieve high performance.

4.1 Scalar control

Scalar Control (SC) is based on the magnitude variation of stator voltage and frequency according to v/f constant rule [33]. The implementation of SC is tranquil but its use for high and wide range of speed control is insufficient and inefficient [20]. Figure 2 elaborates the SC also known as v/f .

The slip-speed ω_s from the controller output in addition with the rotor speed ω_r gives synchronous speed. Synchronous speed along with the voltage command from v/f function maintains the flux at constant value [34, 35].

4.2 Vector control

SC strategy gives poor dynamic response due to the magnitude and phase deviation of air gap flux linkages influencing high performance of drive system [36]. IFOC provides the control of IM like separately excited dc motor [34]. In a dc motor, the decoupled field flux ψ_f and armature flux ψ_a are produced by I_f and I_a , respectively. Torque is controlled by armature current I_a while flux is controlled by field current I_f [14]. With the IFOC scheme, the stator phasor current I_s can be resolved into two components. The horizontal component I_f along rotor flux ψ_r and vertical component I_T generating the required torque [14, 34]. Rotor flux ψ_r can be independently controlled from field current as shown in Fig. 3.

$$I_{ds} = \psi_r \propto I_f \quad (32)$$

Similarly, torque is controlled by torque generating current I_T as follows:

$$T_e \propto \psi_r I_T \propto I_f I_T \quad (33)$$

Field angle θ_f can be obtained as

$$\theta_f = \theta_r + \theta_{sl} \quad (34)$$

where θ_r is rotor angle and θ_{sl} is slip angle.

$$\theta_f = \int (\theta_r + \theta_{sl}) dt = \int (\omega_s) dt \quad (35)$$

4.3 Classification of vector control scheme

Vector control scheme is classified into direct and indirect control schemes on the basis of how field angle is obtained. Field angle acquired using Hall sensors or terminal voltages and currents or by flux sensing windings is recognized as direct vector control scheme. On the other hand, the field angle calculated from rotor position without using current or voltage as variables is recognized as IFOC [14].

Vector control scheme can be broadly classified using Fig. 4 [36].

4.3.1 Indirect vector control scheme

Equation of rotor voltage for squirrel cage induction motor in synchronous frame can be stated as [23,37]:

$$R_r I_{qr} + d\psi_{qr}/dt + \omega_{sl} \psi_{dr} = 0 \quad (36)$$

$$R_r I_{dr} + d\psi_{dr}/dt - \omega_{sl} \psi_{qr} = 0 \quad (37)$$

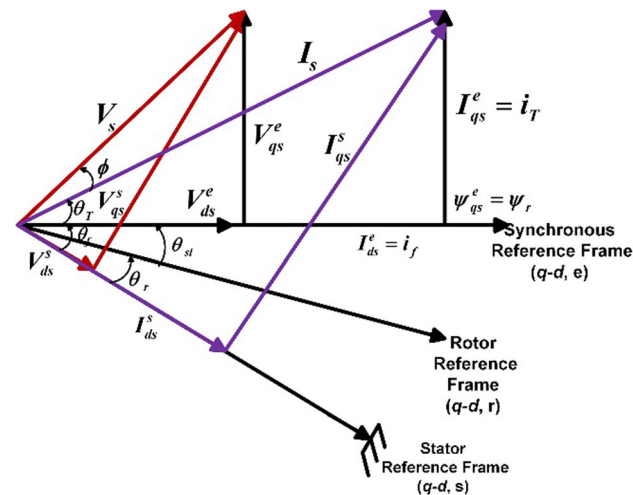
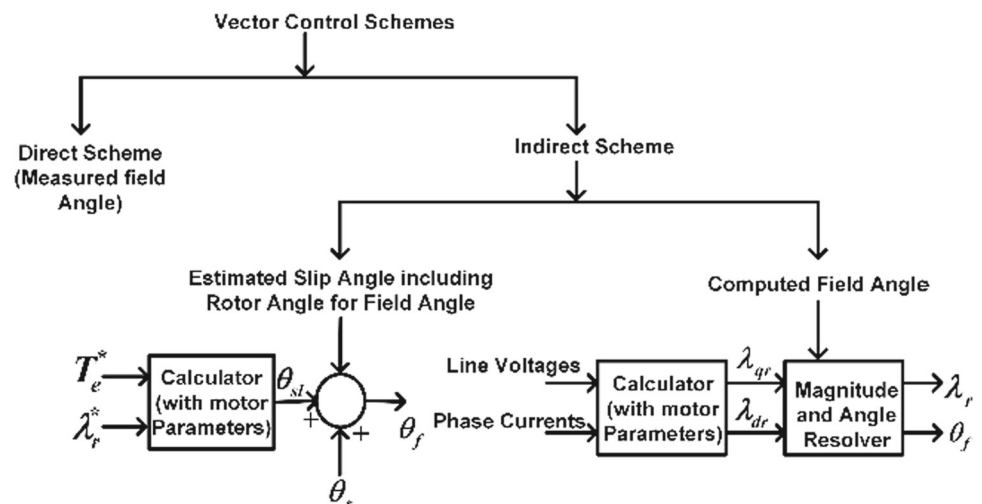


Fig. 3 Indirect vector controller principle

Fig. 4 Classification of vector control schemes



whereas the slip speed can be represented as

$$\omega_{sl} = (\omega - \omega_r) \quad (38)$$

Rotor flux ψ_r equation aligned with d -axis synchronous reference frame can be represented as

$$\psi_r = \psi_{dr}$$

$$\psi_{qr} = 0 \quad \text{and} \quad d\psi_{dr}/dt = 0$$

From the flux linkage equations, rotor currents can be derived as

$$I_{qr} = \frac{-L_m}{L_r} I_{qs} \quad (39)$$

$$I_{dr} = \frac{\psi_r}{L_r} - \frac{L_m}{L_r} I_{ds} \quad (40)$$

The dq -axis stator currents can be obtained by putting ψ_r , ψ_{qr} , I_{qr} and I_{dr} in rotor voltage equations as

$$I_{qs} = \omega_{sl} \frac{L_r \psi_r}{R_r L_m} = I_T \quad (41)$$

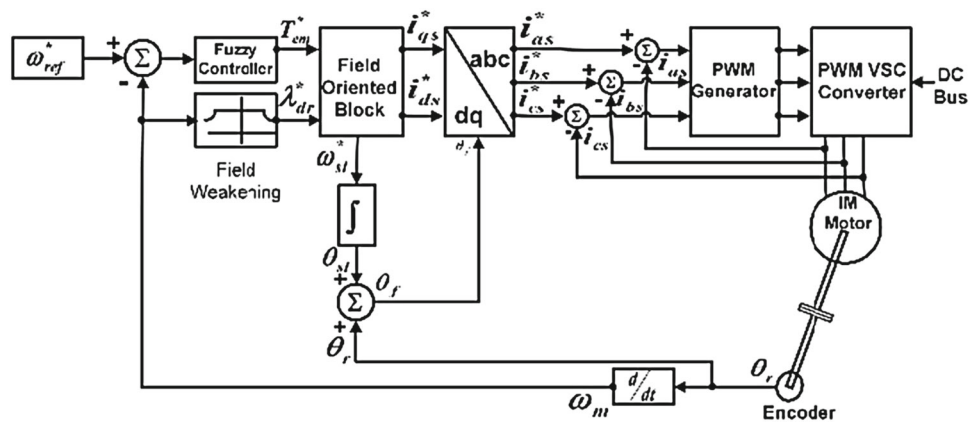
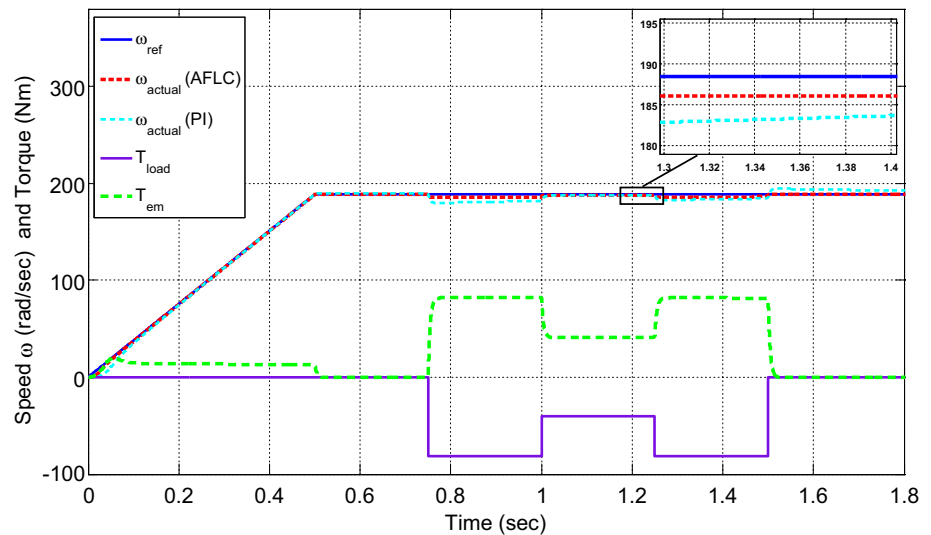
$$I_{ds} = \psi_r + \frac{L_r}{R_r} \frac{d\psi_r}{dt} = I_f \quad (42)$$

$$\omega_{sl} = \frac{L_m R_r I_T}{L_r \psi_r} \quad (43)$$

The d -axis stator current I_{ds} is the field producing component I_f and is in phase with the rotor flux ψ_r , whereas the perpendicular component of stator current I_{qs} is the torque controlling component as shown in Fig. 3.

The stator current phasor can be obtained from the summation of field angle θ_f and θ_r , where

$$\theta_T = \tan^{-1} \left(\frac{I_T}{I_f} \right) \quad (44)$$

Fig. 5 Proposed system block diagram using AFLC**Fig. 6** Rotor speed under variable load torque, a comparison of AFLC based on LM & PI

Electromagnetic torque T_e can be represented as

$$T_e = \frac{3PL_m}{2L_r} \psi_r I_T \quad (45)$$

4.3.1.1. Model for IFOC IM drive

The configuration of the drive investigated in this paper is elaborated in Fig. 5. The system model basic schematic consists of current controlled Pulse Width Modulation (PWM)-based IFOC IM drive. The speed loop is controlled by designed control scheme. Torque is provided by stator current component i_{qs}^* and the flux is generated by stator current component i_{ds}^* . The field angle orientation θ_f is calculated from the sum of rotor angle θ_r and slip angle θ_{sl} by integrating the slip speed. The field-oriented block guarantees the alignment of rotor flux linkages with the d – axis. Moreover, the flux weakening block is also incorporated for variable speed operation.

5 Results and performance evaluation

In this section, the results of the proposed AFLC controller are presented and compared with conventional PI controller. The parameters and control scheme constants are elaborated in Tables 2 and 3 of the appendix. To validate the proposed controller, both controllers were implemented in Simulink/MATLAB along with the IM. The performance of each controller is analyzed by introducing variation in the load torque and reference speed. The tracking ability of the proposed AFLC is much better than the conventional PI controller with better steady- state error and transient response. With load torque and speed variation, AFLC based on LM technique updates its center and variance abruptly to maintain the speed at the desired reference value with low settling time and almost zero steady-state error. In contrast, the PI controller tracks the signal with greater steady state error.

Case 1 (variable load torque, constant speed at rated value)

Fig. 7 dq axis stator currents for both AFLC & PI controller

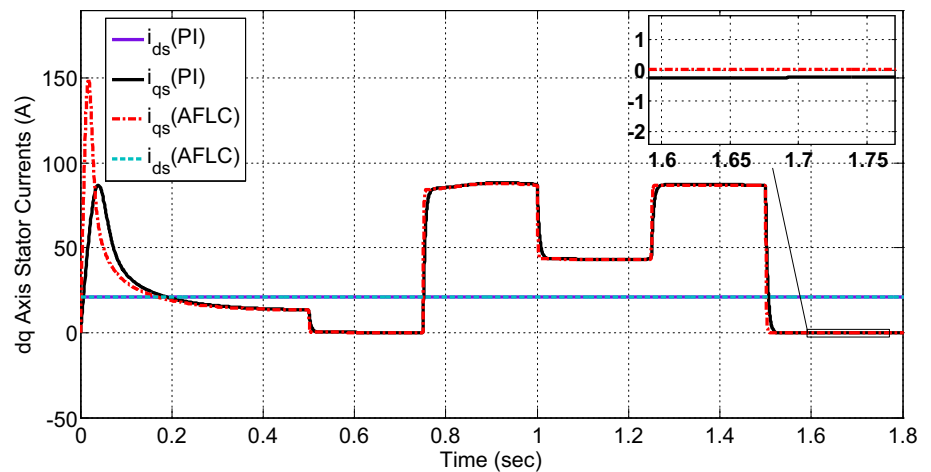
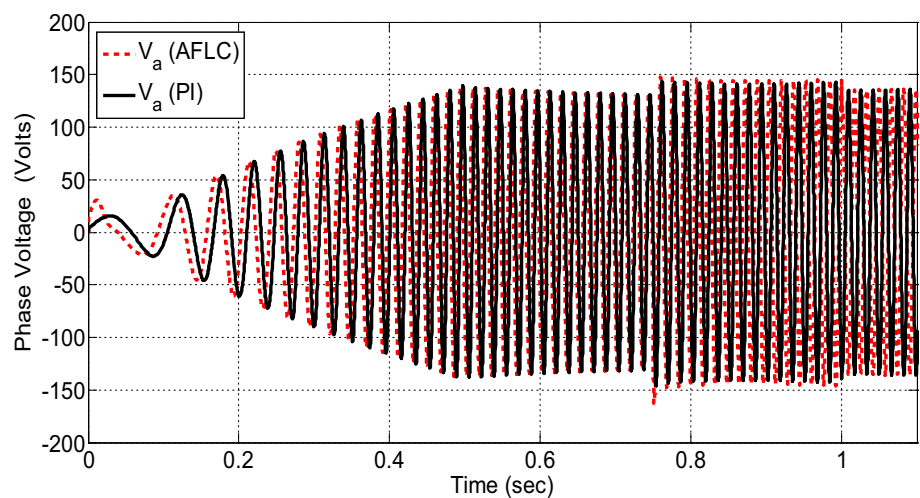


Fig. 8 Stator phase voltage for both AFLC & PI controller

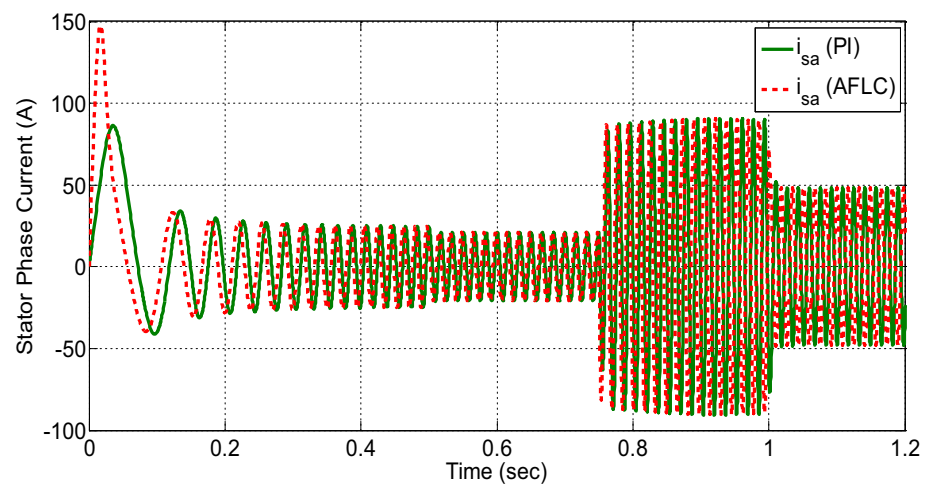
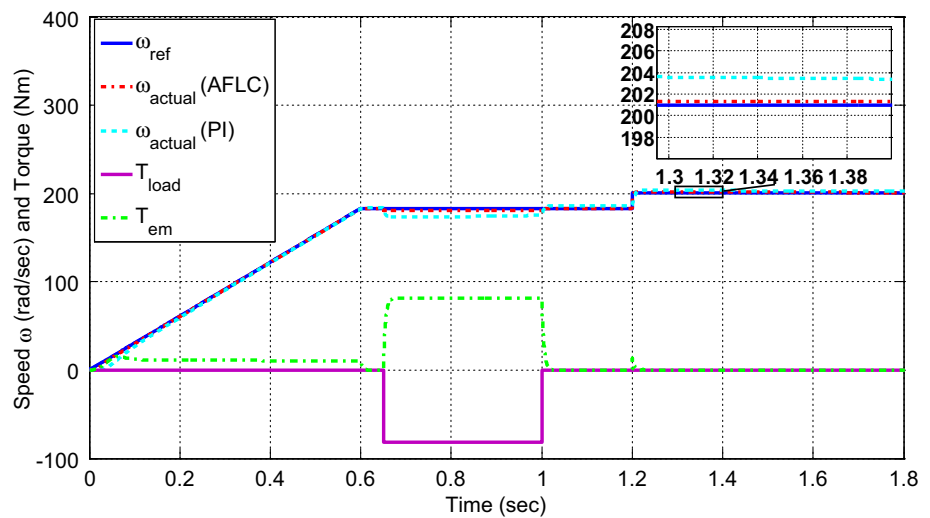


Initially, the motor is stationary with no load condition and reaches rated speed at $t = 0.5$ s. In Fig. 6, when the load torque is varied from 0 to -80 Nm at 0.75 s, the AFLC quickly adjusts its parameters to regulate the motor speed, whereas PI controller requires more time to get back to reference. Similarly, the load torque is varied at $t = 1, 1.25, 1.5$ s to a value of $-40, -80, 0$ Nm, respectively. In all load torque variations, the proposed AFLC shows robustness and continues to track the reference with small steady-state error. In contrast, PI controller takes too much time to get back to the reference speed value and also the steady-state error has significant value. After $t = 1.5$ s, the load torque variation is made zero, but it can be seen from Fig. 6 that the steady-state error of PI is larger than AFLC. Figure 6 shows that AFLC has tracking ability with better steady-state error and transient response than conventional PI controller. The corresponding variation in dq axis stator currents, stator phase voltage and phase current is shown in Figs. 7, 8 and 9, respectively. Figure 7 shows that the AFLC quickly updated its parameters, thereby forcing the q component of current to zero level faster than PI. In steady state, PI does not map the q component

exactly to zero, due to which it does not track the reference speed with zero steady-state error, whereas in case of AFLC the current is aligned to zero line. Similar behavior can be observed in Figs. 8 and 9 where the stator phase voltage and current responses with AFLC lead the responses when compared to those of PI. Due to leading stator voltage, it tracks the reference speed more accurately. The response of AFLC is better because it quickly tracks the desired speed with less steady-state error. The performance of the controller is further evaluated using Integral Absolute Error (IAE), Integral Time-Weighted Error (ITAE) and Integral Square Error (ISE), as shown in Table 1 (case 1). The IAE, ITAE and ISE of AFLC is less than the PI demonstrating that the performance of AFLC is far better than PI.

Case 2 (variation of both load torque and speed)

The effectiveness of the controller is further verified by analyzing its behavior under the variation of both, the load torque and reference speed value. The load torque is varied from 0 to -80 Nm at 0.65 s and at $t = 1$ s, it is again changed to 0 Nm. Similarly, the reference of speed is increased from 183 rad/s to a value of 201 rad/s. The time domain plot

Fig. 9 Stator phase current for both AFLC & PI controller**Fig. 10** Rotor speed under variable load torque, a comparison of AFLC based on LM & PI

of speed and torque for both the controllers is depicted in Fig. 10. The AFLC is much better in maintaining the motor speed at desired reference value than PI. The AFLC quickly updated its parameters and maintained the reference speed even in the presence of load torque variation. In contrast, PI controller significantly deviated from the reference speed value with a large steady state error. Similarly, when the reference speed is increased to 201 rad/s, the AFLC quickly tracked the new reference speed. The PI controller also followed the new reference but with notable steady-state error. Therefore, in both scenarios the AFLC performance is better than conventional PI controller. The corresponding variation in dq axis stator currents, stator phase voltage and phase current is shown in Figs. 11, 12 and 13, respectively. From Fig. 11, it can be seen that when the load torque is changed from -80 to 0 Nm at $t = 1$ s, the AFLC forces the q component to zero level faster than PI controller. Similarly, when the speed is increased from rated value to 201 rad/s, AFLC quickly settled q component to zero as opposed to PI where the overshoot and settling time is greater. Similar behavior

can be seen from Figs. 12 and 13 showing that when the speed is increased, the overshoot in phase voltage and current due to PI controller is greater than that of the proposed AFLC. The reason being the faster response of the AFLC to quickly track the desired speed with less steady-state error.

Case 3 (variation of both load torque and speed—speed varied to half the rated value)

The third case scenario is achieved by introducing similar kind of variation in load torque, but in this case the speed is decreased to one half of the rated value, that is, 91 rad/s. The load torque is varied from 0 to -80 Nm at 0.65 s and at $t = 1$ s, it is reverted to 0 Nm. The reference of speed is decreased from a value of 183 – 91 rad/s. The controller response to follow the abrupt changes in speed and torque is shown in Fig. 14. As the load torque is varied, AFLC immediately adopted the abrupt variation and maintained the reference speed after going through little deviation. In contrast, PI controller deviated from the reference value with a significant large steady-state error as shown in Fig. 14. The performance of PI is not satisfactory even at the point

Fig. 11 dq -axis stator currents for both AFLC & PI controller

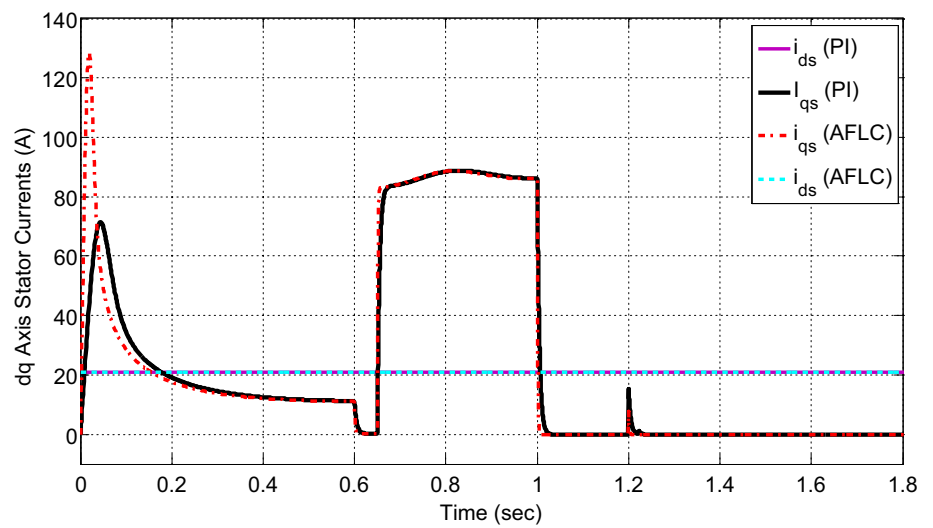


Fig. 12 Stator phase voltage for both AFLC & PI controller

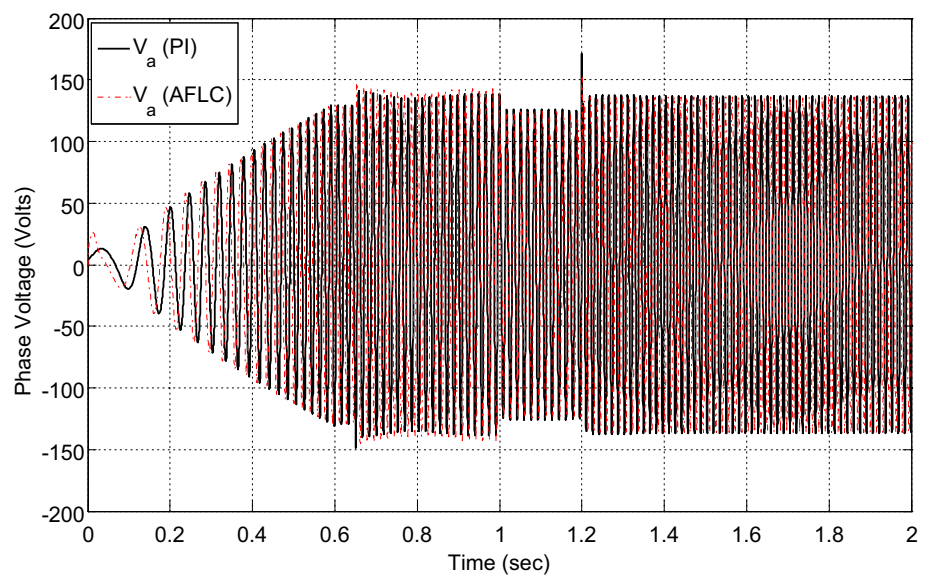


Fig. 13 Stator phase current for both AFLC & PI controller

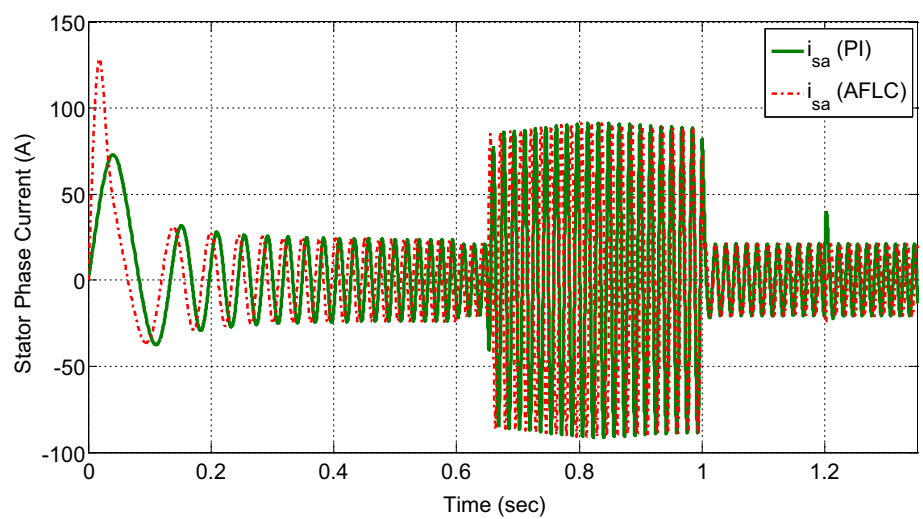


Fig. 14 Rotor speed under variable load torque, a comparison of AFLC based on LM & PI

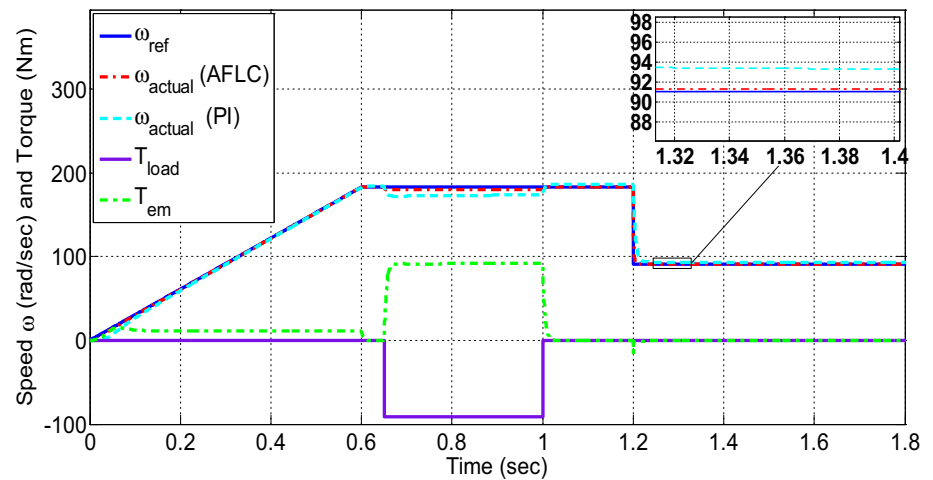


Fig. 15 dq -axis stator currents for both AFLC & PI controller

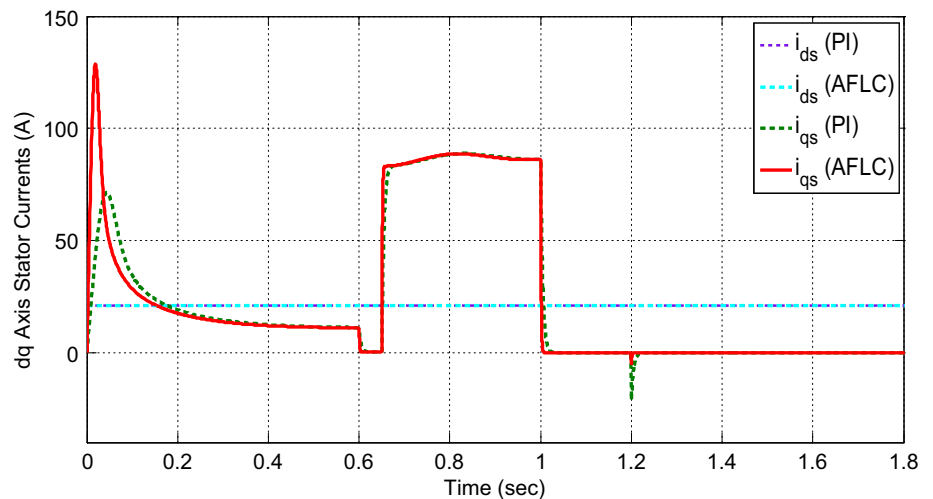
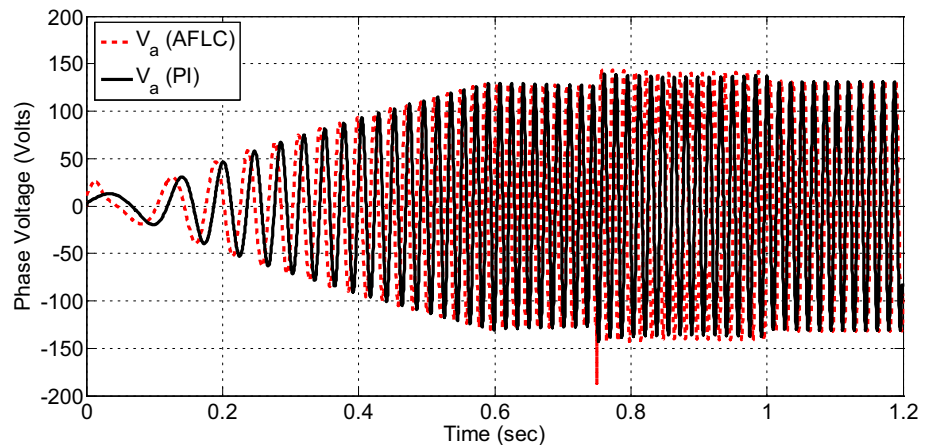
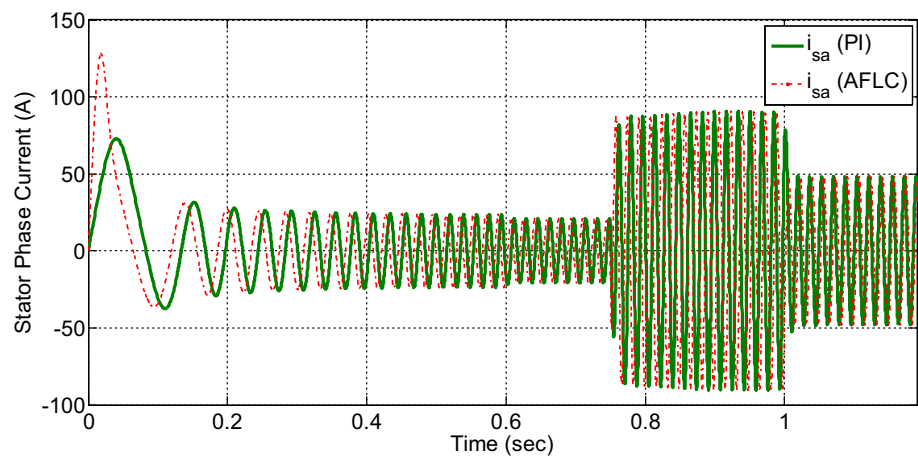


Fig. 16 Stator phase voltage for both AFLC & PI controller



where load torque is reverted to 0 Nm, but AFLC effectively tracked the reference. In a similar manner, when the speed is decreased to one half of rated value, the AFLC tracked the new reference faster than PI and with less steady-state error. Therefore, in both scenarios the AFLC performance is better than conventional PI controller. The corresponding variation

in dq axis stator currents, stator phase voltage and phase current is shown in Figs. 15, 16 and 17, respectively. From Fig. 15, it can be seen that when the load torque is changed from -80 to 0 NM, the q component of current is forced to zero level by AFLC faster than PI controller. Similarly, when the speed is decreased from rated value to 91 rad/s, AFLC

Fig. 17 Stator phase current for both AFLC & PI controller**Table 1** Performance indices IAE and ISE

Case 1 (variable load torque, constant speed at rated value)			
Controller	IAE	ISE	ITAE
PI	7.961	48.51	8.609
AFLC	2.092	3.916	2.106
Case 2 (variation of both load torque and speed)			
Controller	IAE	ISE	ITAE
PI	6.556	37.61	5.987
AFLC	1.543	2.986	1.208
Case 3 (variation of both load torque and speed—speed varied to half the rated value)			
Controller	IAE	ISE	ITAE
PI	6.75	58.57	6.138
AFLC	1.611	7.832	1.281

quickly settled q component to zero as opposed to PI where the overshoot and settling time is greater. Similar behavior can be seen from Figs. 16 and 17 showing that when the speed is decreased, the overshoot in phase voltage and current due to PI controller is greater than the proposed AFLC. The reason being the faster response of the AFLC to quickly track the desired speed with less steady-state error.

The performance of controller is further evaluated using Integral Absolute Error (IAE), Integral Time-Weighted Error (ITEA) and Integral Square Error (ISE), as shown in Table 1 (case 3). The IAE, ITAE and ISE of AFLC is less than the respective of PI demonstrating that the performance of AFLC is far better than PI.

6 Conclusion

In this paper, an Indirect Field-Oriented Control (IFOC) scheme for a drive system of three-phase induction motor

is effectively investigated and validated using various simulation results in Matlab/Simulink. The performance of proposed controller is verified by introducing variation in speed and load torque. Simulation results demonstrate that PI has sluggish response compared to AFLC. In all load torque variations, the proposed AFLC shows robustness and continues to track the reference with small steady-state error. Moreover, AFLC based on LM is robust to model parameter variations, load variations and less sensitive to uncertainties and disturbances. The proposed scheme verifies superior and smoother performance with improved dynamic response. Furthermore, the effectiveness of proposed AFLC is evaluated and justified from performance indices IAE, ISE and ITAE.

7 Appendix

See Tables 2 and 3.

Table 2 Design controller constants

Controller	Constants	Values
PI controller	k_p	30
	k_i	7
AFLC based on LM	b_1	0.1
	b_2	0.08
	c_1	0.7
	c_2	0.8
	σ_1	0.03
	σ_2	0.5
	λ	0.2
	μ	0.69

Table 3 Machine nominal parameters

IM parameters	Values
Rated Power	20 hp
Voltage	220V ($-L, rms$)
Phases	3
System frequency	60 Hz
Full load Slip	0.0287
Number of poles	4
Stator resistance	0.1062 Ω
Rotor resistance	0.0764 Ω
Stator leakage resistance	0.2145 Ω
Rotor leakage resistance	0.2145 Ω
Inertia	2.5 kgm ²

References

- Leonhard W (1996) Controlled AC drives, a successful transfer from ideas to industrial practice. *Control Eng Pract* 4(7):897–908
- Fitzgerald AE, Kingsley CU, Stephen D (1990) *Electric machinery*, 5th edn. McGraw-Hill, New York
- Marino R, Peresada S, Valigi P (1993) Adaptive input-output linearizing control of induction motors. *IEEE Trans Autom Cont* 38(2):208–221
- Leonhard W (1985) *Control of electrical drives*. Springer, Berlin
- Heinemann G (1989) Comparison of several control schemes for ac induction motors. In: *Proceedings of European Power Electronics Conference (EPE'89)*, pp 843–844
- Bose BK (1984) Scalar decoupled control of induction motor. *IEEE Trans Ind Appl IA*–20(1):216–225
- Jung J, Nam K (1998) A vector control schemes for EV induction motors with a series iron loss model. *IEEE Trans Ind Electron* 45:617–624
- Blaschke F (1972) The principle of field orientation as applied to the new transvector closed-loop control system for rotating-field machines. *Siemens Rev* 34(5):217–219
- Hasse K (1968) Zum Dynamischen Verhalten der Asynchronmaschine bei Betrieb Mit Variabler Ständerfrequenz und Ständerspannung. *ETZ-A* 89:387–391
- Boldea BL, Nasar SA (1992) *Vector control of AC drives*. CRC Press, Boca Raton
- Zhang Y, Jiang Z, Yu X (July 2008) Indirect field-oriented control of induction machines based on synergetic control theory. In: *Proceedings of the IEEE International Conference on Power and Energy Society General*, pp 20–24
- Bose BK (1997) *Power electronics and variable frequency drives*. IEEE press standard publishers, New York
- Krishnan R (2002) *Electric motors drives modeling analysis and control*. Publication Prentice Hall of India, Upper Saddle River
- Lee C (1990) Fuzzy logic in control systems: fuzzy logic controller part 1. *IEEE*, New Delhi
- Lee C (1990) Fuzzy logic in control systems: fuzzy logic controller part 2. *IEEE*, New Delhi
- Kouzi K, Mokrani L, Nait-Said MS (2003) A new design of fuzzy logic controller with fuzzy adapted gains based on, indirect vector control for induction motor drive. In: *IEEE proceedings of the 35th southeastern symposium on system theory*, pp 362–366
- Beierke S, Altrock C (1996) Fuzzy logic enhanced control of an induction motor with DSP. In: *5th IEEE international conference on fuzzy systems*, New Orleans, LA
- Spiegel RJ, Turner MW, McCormick VE (2003) *Fuzzy sets and systems*. Elsevier, New Jersey, pp 387–401
- Krause P, Wasynczuk O, Sudhoff S (2002) *Analysis of electric machinery and drive systems*, 2nd edn. Wiley, New Jersey
- Chee-Mun Ong (1998) *Dynamic simulation of electric machinery using MATLAB/Simulink*, 1st edn. Prentice Hall PTR, New Jersey
- Wu B, Lang Y, Zargari N, Kouro S (2011) *Power conversion and control of wind energy systems*. Wiley, New Jersey
- Eltamaly AM, Alolah AI, Basem MB (2010) Fuzzy Controller for Three Phases Induction Motor Drives. In: *International conference on Autonomous and Intelligent Systems (AIS)*, pp 1–8
- Pedrycz W (1989) *Fuzzy control and fuzzy system*. Wiley, New York
- Wilamowski BM, Yu H (2010) Improved computation for Levenberg-Marquardt training. *IEEE Trans Neural Netw* 21:930–937
- Yu H, Wilamowski BM (2011) Levenberg-Marquardt Training. *The Industrial Electronics Handbook*- eng.auburn.edu, pp (12-1)–(12-16)
- Wilamowski BM, Yu H (2010) Improved computation for Levenberg-Marquardt training. *IEEE Trans Neural Netw* 21(6):930–937
- Huang YL, Lou HH, Gong JP, Edgar TF (2000) Fuzzy model predictive control. *IEEE Trans Fuzzy Syst* 8(6):665–678
- Wang HO, Tanaka K, Griffin MF (2002) An approach to fuzzy control of nonlinear systems: stability and design issues. *IEEE Trans Fuzzy Syst* 4(1):14–23
- Jeffrey T, Spooner, Kevin M (1996) Stable adaptive control Using fuzzy systems and neural networks. *IEEE Trans Fuzzy Syst* 4(3):339–359
- Levenberg K (1944) A method for the solution of certain problems in least square. *Q Appl Math* 2:164–168
- Marquardt D (1963) An algorithm for least-squares estimation of nonlinear parameters. *Society Ind Appl Math J Appl Math* 11:431–441
- Harbour JP (2001) Evaluation and comparison of electric propulsion motors for submarines. Master dissertation, Massachusetts Institute of Technology. <http://calhoun.nps.edu/handle/10945/10910>
- Bose BK (2002) *Modern power electronics and AC drives*. Prentice-Hall, Upper Saddle River
- Betin F, Depermet D, Floczek P, Faqir A, Lanfranchi V, Pinchon D, Goeldel C, Capolino A (2001) Fuzzy logic scalar control for induction machine drive: comparison with classical drive. In: *International AEGERAN conference on electrical machines and power electronics*, pp 27–29
- Gopakumar K, Sathiakumar S, Biswas SK, Vithayathil J (1984) Modified current source inverter fed induction motor drive with reduced torque pulsations. *Proc Inst Elect Eng B* 131(4):159–164
- Krishnan R, Doran FC (1987) Study of parameter sensitivity in high performance and inverter-fed induction motor drive systems. *IEEE Ind Appl IA*–23(4):623–635
- Mohan N (2001) *Advance electric drives analysis, control and modeling using Simulink*. MNPERE, Ney Jersey